

## Halogen Bonding—A Novel Interaction for Rational Drug Design?

Yunxiang Lu,<sup>\*,†</sup> Ting Shi,<sup>†</sup> Yong Wang,<sup>†</sup> Huaiyu Yang,<sup>†</sup> Xiuhua Yan,<sup>†</sup> Xiaoming Luo,<sup>†</sup> Hualiang Jiang,<sup>†</sup> and Weiliang Zhu<sup>\*,†,‡</sup>

Drug Discovery and Design Center, Shanghai Institute of Materia Medica, Chinese Academy of Sciences, Shanghai 201203, China, and School of Science, East China University of Science and Technology, Shanghai, 200237, China

Received January 7, 2009

Although recognized in small molecules for quite some time, the implications of halogen bonding in biomolecular systems are only now coming to light. In this study, several systems of proteins in complex with halogenated ligands have been investigated by using a two-layer QM/MM ONIOM methodology. In all cases, the halogen–oxygen distances are shown to be much less than the van der Waals radius sums. Single-point energy calculations unveil that the interaction becomes comparable in magnitude to classical hydrogen bonding. Furthermore, we found that the strength of the interactions attenuates in the order  $H \approx I > Br > Cl$ . These results agree well with the characteristics discovered within small model halogen-bonded systems. A detailed analysis of the interactions reveals that halogen bonding interactions are responsible for the different conformation of the molecules in the active site. This study would help to establish such interaction as a potential and effective tool in the context of drug design.

### Introduction

Intermolecular forces have been the subject of intense interest from both experimental and theoretical points of view due to their fundamental role in determining the three-dimensional structure of a wide number of important molecules such as proteins, DNA, and enzyme–substrate complexes. Hydrogen bonding, the most common and important type of weak interaction, has been extensively studied over the past several years. Recently, a specific molecular interaction where halogen atoms act as electrophiles is under active investigation.<sup>1</sup> Such interaction is now referred to as halogen bonding to emphasize their characteristics in parallel with those of hydrogen bonding in terms of strength and directionality.<sup>2</sup>

The ability of halogen atoms to function as general, effective, and reliable sites for directing molecular recognition processes was completely ignored until the 1990s. During the past decade, many applications of halogen bonding in fields as diverse as crystal engineering, enantiomer's separation, and supermolecular architectures were reported and reviewed.<sup>2–8</sup> For example, the potential of the interaction shown in the design of novel and high-value engineering functional materials was overviewed in detail by Resnati and co-workers.<sup>3–5</sup> They also pointed out that halogen bonding has an impact on all areas where the control of intermolecular recognition and self-assembly processes plays a central role. Some other research groups have explored the competition between hydrogen bonding and halogen bonding in molecular assemblies, and more importantly, effective supermolecular synthetic strategies around a hierarchy of synthons that comprise both hydrogen bonding and halogen bonding through systematic cocrystallization reactions were preliminarily developed.<sup>9</sup> Very recently, Dutremez et al. have reported the structural characterization of molecular assemblies constructed from imidazolyl-containing haloalkenes and haloalkynes and found that  $N \cdots I$  halogen bonding interactions

observed in certain systems were shown not to be presented as the arrangement of the molecules is governed by two interwoven hydrogen bonding networks.<sup>10</sup>

Albeit recognized in small molecules for quite some time, the implications of halogen bonding, or halogen to oxygen (or nitrogen) interactions that are equal to or below the van der Waals radius sums in biological molecules, are only, nowadays, coming to light.<sup>3,11–20</sup> These short contacts have rarely been observed in biological systems, probably because of the scarcity of available crystal structures of halogenated biomolecules to date. Halogens do, however, play crucial roles in natural systems. The peculiar chemical features of halogens render them very useful in designing protein inhibitors and drugs; about half of the molecules applied in high-throughput screening are halogenated. The importance of halogen bonding in the field of biology was first recognized by Ho and co-workers, and in a pioneering work, they have characterized the prevalence and geometry of halogen bonds ( $X \cdots O$  interactions) in biological systems.<sup>11</sup> One example of the use of halogen bonding in drug design was the development of 4-(3,5-dimethylphenoxy)-5-(furan-2-ylmethylsulfanylmethyl)-3-iodo-6-methylpyridin-2(1H)-one (R221239),<sup>15</sup> a pyridinone derivative, which strongly inhibits wild type human immunodeficiency virus-1 (HIV-1<sup>cr</sup>) reverse transcriptase and drug-resistant variants, including Tyr181Cys and Lys103Asn mutants. This compound contains an iodine atom that forms a halogen bond with the Tyr188 carbonyl oxygen; this interaction was regarded as one of the important interactions leading to the overall protein–ligand binding affinity.<sup>15</sup>

The current Protein Data Bank (PDB) (December 2008 release) contains over 1000 structures in which the ligands are

\* To whom correspondence should be addressed. For W.L.Z.: phone, +86-21-50805020; fax, +86-21-50807088; E-mail, wlzhu@mail.shnc.ac.cn. For Y.X.L.: phone, +86-21-50806600 ext 1201; fax, +86-21-50807088; e-mail, lu\_yunxiang@163.com.

<sup>†</sup> Drug Discovery and Design Center, Shanghai Institute of Materia Medica, Chinese Academy of Science.

<sup>‡</sup> East China University of Science and Technology.

<sup>a</sup> Abbreviations: HIV-1, human immunodeficiency virus-1; ATP, adenosine triphosphate; QM/MM, quantum mechanics/molecular mechanics; ONIOM, our own N-layered integrated molecular orbital and molecular mechanics; JNK3, c-Jun terminal kinase 3; CDK2, cyclin-dependent kinase 2; CK2, cyclin kinase 2; MEK1/2, mitogen-activated protein kinase kinase 1/2; GRP94, glucose-regulated protein 94; ART, adenosine diphosphate-ribosyl transferase; AK, adenosine kinase; hTR $\beta$ , human thyroid hormone receptor; DFT, density functional theory; RESP, restricted electrostatic-potential; GAFF, generalized amber force field; BSSE, basis set superposition error; TBB, tetrabromo-benzimidazole; rmsd, root-mean-square deviation; T4, thyroxine; T3, triiodothyronine.

**Table 1.** Summary of Halogen Bonds in Selected Protein–Ligand Complexes

proteins	ligands	PDB ID	resolutions, Å	IC <sub>50</sub>	halogens <sup>a</sup>	electron donors <sup>b</sup>	<i>d</i> (X···O), Å	∠(C–X···O), deg	∠(C–O···X), deg
Protein Kinase Systems									
JNK3	compd 1 <sup>53</sup>	1PMN	2.20	7 nM	Cl1	Ala91 O	2.83	159	96
CDK2	NU6086 (2) <sup>54</sup>	1H1R	2.00	2.3 μM	Cl1	Asp86 O	2.84	140	110
CK2	K37 (3) <sup>55</sup>	1ZOG	2.30	250 nM	Br1	Val116 O	2.98	175	130
	K44 (4) <sup>55</sup>	1ZOH	1.81	740 nM	Br2	Glu114 O	3.23	144	162
					Br1	Val116 O	2.89	177	129
					Br2	Glu114 O	3.18	145	164
MEK1	PD318088 (5) <sup>56</sup>	1S9J	2.40	—	II	Val127 O	3.13	174	129
MEK2	PD334581 (6) <sup>56</sup>	1S9I	3.20	—	II	Val131 O	3.17	176	118
Other Systems									
GRP94	2Cldda <sup>57</sup>	1QYE	2.10	—	Cl1	Gly153 O	2.92	142	101
ART	BNA <sup>58</sup>	1GXZ	2.10	—	Br1	Gln187 O	3.16	169	122
AK	7-iodotubercidin <sup>59</sup>	1LJ	1.86	—	II	Thr45 O	3.34	149	108
hTRβ	T3 <sup>60</sup>	1NQ2	2.40	—	II	Phe272 O	3.07	171	120

<sup>a</sup> The numbering of halogens is defined in Figure 1. <sup>b</sup> Asp O is the side chain oxygen, while others are backbone carbonyl oxygen.

halogenated. From these structures, we collected those with X···O distances that are less than their respective van der Waals radius sums,<sup>21</sup> i.e.,  $d(\text{Cl}\cdots\text{O}) < 3.27 \text{ \AA}$ ,  $d(\text{Br}\cdots\text{O}) < 3.37 \text{ \AA}$ , and  $d(\text{I}\cdots\text{O}) < 3.50 \text{ \AA}$ , as well as with halogen bonding angles,  $\angle(\text{C}-\text{X}\cdots\text{O})$ , that are larger than 140°. It was found that 154 protein structures associated with halogen-oxygen contacts satisfy the criteria, leading to a total of 248 distinct X···O interactions, as summarized in Supporting Information. The amount of X···O interactions increased by more than one time compared to those assembled in 2004 with a less standard angle criterion,  $\angle(\text{C}-\text{X}\cdots\text{O}) \geq 120^\circ$ .<sup>11</sup> We, consequently, believe that more and more X···O interactions will be identified along with the enlarged number of halogenated biomolecules. Similar to those observed in 2004, present database includes 47% Cl···O, 22% Br···O, and 31% I···O interactions with backbone carbonyl oxygens or side chain hydroxyl and carboxyl oxygens. Noteworthy, there are 39 halogen bonds, about one-sixth of total X···O contacts, in 24 structures of protein kinases in complex with halogenated ligands.

Protein kinases mediate most of the signal transductions in eukaryotic cells and also control many other essential cellular processes, from metabolism and cell cycle progression to differentiation and apoptosis.<sup>22</sup> The broad variety of function associated with protein kinases has made them the major drug targets of the twenty-first century, with utilization as immunosuppressants and to treat a number of diseases such as cancer, diabetes, and inflammation.<sup>23–25</sup> Protein kinases share a catalytic domain conserved in sequence and structure; the overall structure can be divided into two distinct lobes: the N-terminal lobe consists of a β-sheet and at least one α-helix, while the C-terminal lobe is mostly helical (see Figure 2 as a representative structure).<sup>26</sup> The adenosine triphosphate (ATP) binding pocket is between the two lobes that are connected via the hinge region. This site, together with less conserved surrounding pockets, has served as targets for the design of protein selective inhibitors and drugs.<sup>26</sup> As mentioned above, halogen substitution is an important approach for drug design. Nonetheless, the accurate chemical and structural basis for their contribution to drug–protein affinity and recognition has been largely overlooked and hence has not been fully exploited for rational drug design. More recently, Ho and Voth have surveyed 12 single crystal structures of protein kinase complexes with halogenated molecules and concluded that halogen bonds play important roles in inhibitor recognition and binding based only on a qualitative analysis.<sup>17</sup> Therefore, understanding the nature and strength of halogen bonding in biological systems and identifying the contribution of halogens to the overall effectiveness of

the inhibitors would be very helpful in aiding new protein design and drug discovery.

Halogen bonding within small model systems has been thoroughly studied by means of high level quantum chemical methods.<sup>27–41</sup> The key geometrical and energetic properties of the interaction are fairly well established. For example, the attractive nature of the interaction gives rise to halogen bonding lengths shorter than the sum of van der Waals radii of involved atoms; the strength of the interaction decreases in the following order I > Br > Cl. For large molecules of biological relevance, however, it is not feasible to apply full quantum chemical treatment and still no theoretical works concerning halogen bonding in biomolecules has been reported to our knowledge. The large size of biological systems prohibits the efficient use of electronic structure methods with a reasonable computational cost. At present, the strategy widely applied to investigate biomolecular systems is known as the combined quantum mechanics/molecular mechanics (QM/MM) method,<sup>42</sup> e.g., our own N-layered integrated molecular orbital and molecular mechanics (ONIOM) method introduced by Morokuma and co-workers.<sup>43–45</sup> The advantage of using the ONIOM methodology is that a large biologically relevant system can be partitioned into two layers: the most important part of the system, involving “active-site” atoms, can be treated with accurate QM methods, while the remaining part can be calculated using MM methods. The ONIOM method has currently been proved to be a powerful and practical tool in the study of several enzymatic systems.<sup>46–52</sup>

In the present work, a two-layer ONIOM-based QM/MM approach was employed for the study of protein–ligand complexes. For this purpose, six representative systems of protein kinases, including c-Jun terminal kinase 3 (JNK3), cyclin-dependent kinase 2 (CDK2), cyclin kinase 2 (CK2), and mitogen-activated protein kinase kinase 1/2 (MEK1/2), in complex with small molecule inhibitors, were selected. Also considered are other four systems of glucose-regulated protein 94 (GRP94), adenosine diphosphate–ribosyl transferase (ART), adenosine kinase (AK), and human thyroid hormone receptor (hTRβ) with their halogenated ligands. In all cases, halogen atoms in the ligands form halogen bonds with the backbone carbonyl oxygen of residues Ala, Val, Glu, Gln, Gly, Thr, and Phe, or with the side-chain carboxyl oxygen of residue Asp, as shown in Table 1. The major objective of this work is to provide some insights into the origin and magnitude of halogen bonding in biological systems and, in particular, to compare with those found within small model systems that have been extensively examined. This study would help to clarify how halogen bonds

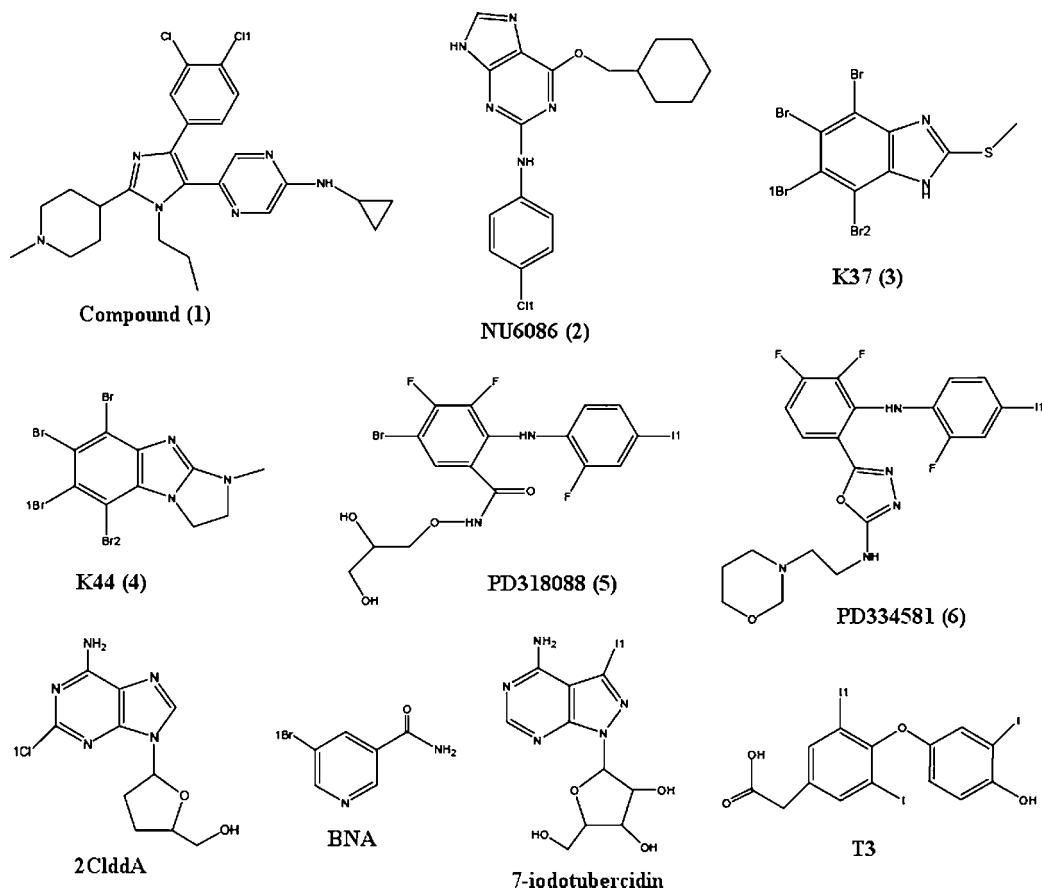


**Figure 1.** Chemical structures of the ligands.

participate in ligand binding and how they can potentially be used in rational drug design.

### Computational Methods

The model systems used here were chosen from the reported data of protein complexes with halogenated ligands, and the structures were built on the basis of the corresponding X-ray crystal structures deposited in the Protein Data Bank (PDB codes: 1PMN,<sup>53</sup> 1H1R,<sup>54</sup> 1ZOG,<sup>55</sup> 1ZOH,<sup>55</sup> 1S9J,<sup>56</sup> 1S9I,<sup>56</sup> 1QYE,<sup>57</sup> 1GXZ,<sup>58</sup> 1LIJ,<sup>59</sup> and 1NQ2<sup>60</sup>). The chemical geometries of the small molecule ligands are systematically depicted in Figure 1. Because there are two almost identical protein complexes in the PDB files of 1H1R, 1S9I, and 1GXZ, we removed one of them by deleting the B chain for 1S9I and 1GXZ and the B (cyclin A3), C, and D (cyclin A3) chains for 1H1R. The normal valency of the atoms in all the model systems was satisfied by adding exact number of hydrogen atoms.

The main goal of this work is to understand the characteristics of halogen bonding in biological systems. To achieve this, the whole systems for the ONIOM-based QM/MM optimizations were segmented into two layers: the ligands and the corresponding protein residues that form halogen bonds with the ligands were in the QM layer (see Figure 4), while the rest atoms were in the MM layer. Hydrogen atoms were used as link atoms to saturate the dangling bonds. For the QM layer, two different density functional theory (DFT) methods were adopted: one is the widely used B3LYP<sup>61,62</sup> method, the other is MPWLYP,<sup>62,63</sup> which has been testified to provide accuracies close to high level correlated ab initio methods in a very recent benchmark study of halogen bonding.<sup>64</sup> The standard 6-31G(d) basis set was applied for 1PMN, 1H1R, 1ZOG, 1ZOH, 1QYE, and 1GXZ, while for 1S9J, 1S9I, 1LIJ, and 1NQ2, the lan12dz basis set was used. The MM layer of the systems was treated by means of the AMBER parm96 force field, and the water molecules were described by the TIP3P model.<sup>65</sup> The restricted



**Figure 2.** The structure of the catalyst domain of JNK3 in complex with 1 as a representative case.

electrostatic-potential (RESP) fitting procedure was employed to obtain partial atomic charges of the ligands, and the generalized amber force field (GAFF) package<sup>66</sup> was used for parameters not found in AMBER force field.

The structures of the model systems were fully optimized based on the two-layer ONIOM-based QM/MM methodology described above without any constraints. The electrostatic interactions between the two layers were treated in terms of mechanical embedding scheme to save computational cost. The optimizations of the model structures are in principle capable of calculating halogen bonding

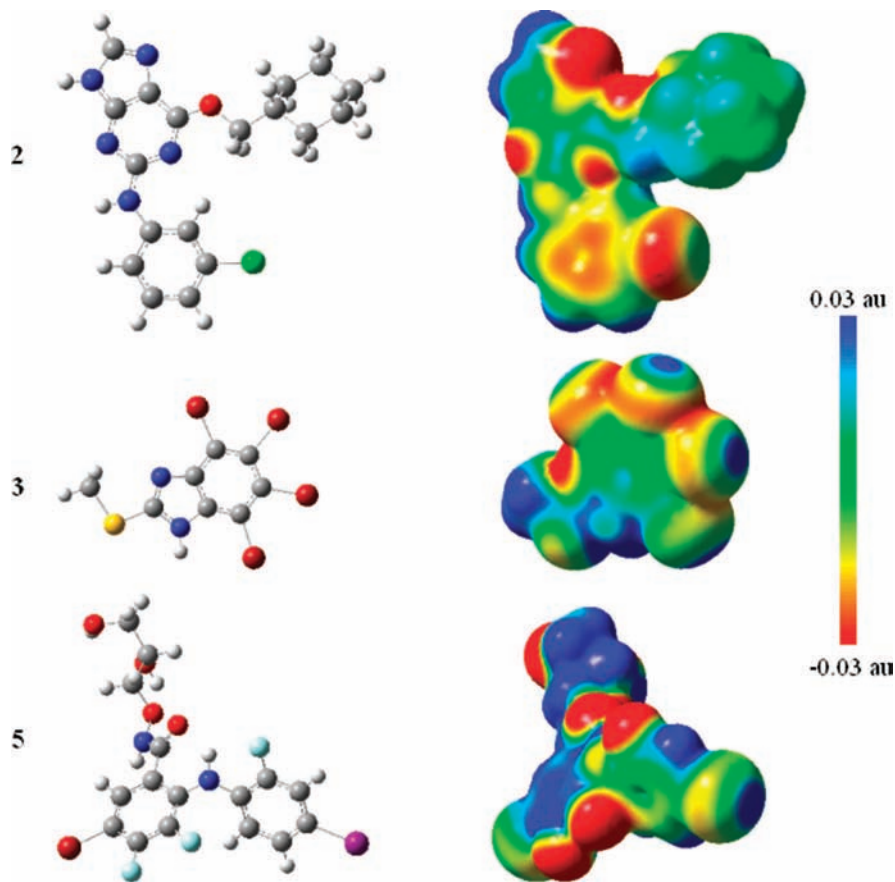


**Figure 3.** The electrostatic potential mapped on the surface of molecular electron density ( $0.02 e \text{ au}^{-3}$ ). The electrostatic potential varies between  $-0.03$  (red) to  $0.03$  (blue) au.

energies. For this aim, the QM layer of the model was selected for single-point energy computations, which were performed at the B3LYP(MPWLYP)/6-311+G(d) level for the systems 1PMN, 1H1R, 1ZOG, 1ZOH, 1QYE, and 1GXZ, and at the B3LYP(MPWLYP)/lanl2dz level for 1S9J, 1S9I, 1LIJ, and 1NQ2. The binding energies between the ligands and protein residues including basis set superposition error (BSSE) corrections<sup>67</sup> were assessed from eq

$$\Delta E = E_1 - (E_2 + E_3) + \text{BSSE} \quad (1)$$

where  $\Delta E$  is the binding energies,  $E_1$  is the energies of the QM layer of the full models,  $E_2$  is the energies of ligands in the QM layer, and  $E_3$  is the energies of QM layer of the protein residues. All of these calculations were carried out with the help of Gaussian 03 suite of programs.<sup>68</sup>

## Results and Discussion

The graphical illustration of electrostatic potential surfaces for three ligands, viz. **2**, **3**, and **5**, is depicted in Figure 3. It is obvious that a small positive electrostatic potential cap is shown at the end region of halogen atoms along the C–X axis, which is surrounded by an electroneutral area and, farther out, a large electronegative domain. An electronegative atom (or group) tends to approach the positive cap, thereby giving rise to a linear interaction. From Figure 3, we can also see a clear tendency of increasing positive cap upon going from Cl to Br and further to I within halogenated compounds. In recent articles, Murray et al. termed the positive cap of halogen atoms as “sigma-hole” that intersects the C–X axis and also extended this concept to atoms of Group V and VI to explore their ability to form directional nonbonded interactions.<sup>69–73</sup>

The optimized structures of the QM layer of the full models for protein kinase systems at the level of ONIOM(B3LYP:AMBER) are given in Figure 4. Halogen atoms in the ligands interact with the backbone carbonyl oxygen of residues Ala, Val, Glu, Gly, Gln, Thr, and Phe, with the exception of 1H1R, in which the Cl atom forms a halogen bond with the side chain carboxyl oxygen of residue Asp. Interactions in the former cases belong to conventional halogen bonds, whereas in the latter, the interaction should be classified as charge-assisted halogen bonds. Note that two of Br atoms in **3** and **4**, selective tetrabromo-benzimidazole (TBB) derivatives, interact with the backbone oxygens of residues Glu114 and Val116, respectively. The geometrical parameters of halogen bonds in the studied systems and the root-mean-square derivation (rmsd) values of the QM layer of the models relative to their X-ray structures at different levels are summarized in Table 2. It can be seen that the interatomic X...O contacts are predicted to be within a range of 2.771–3.173 Å and 2.741–3.143 Å at the B3LYP and MPWLYP levels of theory, respectively. These separations are significantly smaller than the sums of van der Waals radii of the atoms involved.<sup>21</sup> Inspection of Tables 1 and 2 reveals that the calculated halogen bonding lengths are roughly consistent with the experimentally determined values. For example, the distances between the I and O atoms for 1S9J and 1S9I are computed to be 3.068 and 3.173 Å, respectively, via the B3LYP/lanl2dz method, while at the MPWLYP/lanl2dz level, the corresponding distances are 2.981 and 3.111 Å, respectively. These predicted separations reproduce the experimentally measured values (3.134 and 3.165 Å) reasonably well. In addition, the differences of the distances obtained at the two levels are quite limited (less than 0.1 Å), albeit the MPWLYP optimizations fail to converge for the

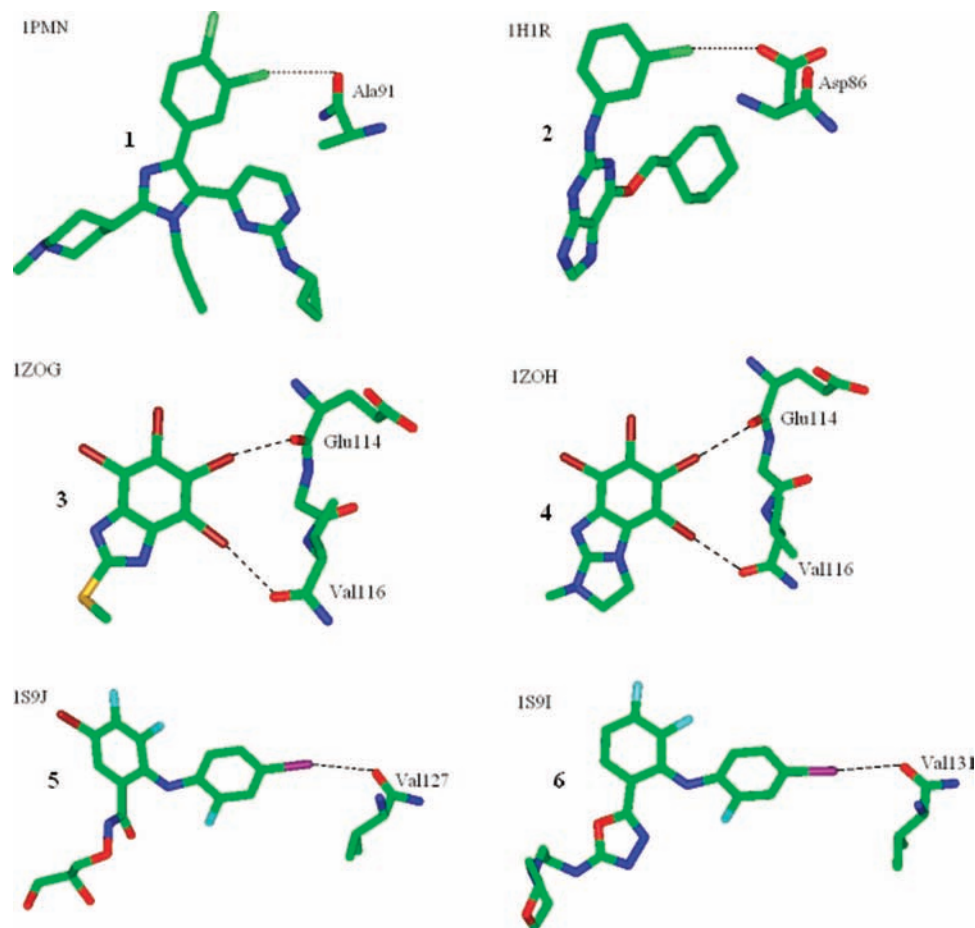


**Figure 4.** Optimized structures of the QM layer of the full models at the ONIOM(B3LYP:AMBER) level.

**Table 2.** Geometrical and Energetic Parameters of Studied Systems and the rmsd Values of the Full Models Relative to X-ray Structures at Different Levels

systems	$d(X\cdots O)$ , Å		$\angle(C-X\cdots O)$ , deg		$\angle(C-O\cdots X)$ , deg		rmsd (QM)		$\Delta E$ (kcal/mol)	
	B3LYP	MPWLYP	B3LYP	MPWLYP	B3LYP	MPWLYP	B3LYP	MPWLYP	B3LYP	MPWLYP
Protein Kinase Systems										
1PMN	2.966	2.967	157.5	155.8	95.2	96.2	2.828	2.837	2.75	2.07
IH1R	2.771	2.741	153.1	152.6	150.0	148.9	1.944	1.966	0.34	-0.98
	2.892		174.8	—	128.3	—	2.034	—	-0.22	—
IZOG	3.168	not converged	163.9	—	144.1	—				
IZOH	2.983		160.5	—	138.0	—	0.818	—	-2.13	—
	2.932	not converged	170.4	—	127.2	—				
1S9J	3.068	2.981	165.4	167.0	133.7	128.8	2.550	2.387	-1.60	-1.90
1S9I	3.173	3.111	172.2	174.6	137.1	137.4	2.355	2.360	-1.96	-3.05
Other Systems										
1QYE	3.060	3.092	147.4	148.2	98.0	95.3	0.213	0.225	0.89	0.18
1GXZ	3.032	3.020	149.2	148.2	123.6	123.4	0.360	0.371	2.05	1.36
1LJ	3.151	3.143	155.5	153.2	122.2	120.1	2.231	2.245	-1.39	-2.02
1NQ2	3.000	3.109	170.8	174.6	120.0	122.5	2.643	2.648	-1.66	-3.22

systems of IZOG and IZOH. The calculated halogen bonding energies show, however, a distinct discrepancy between B3LYP and MPWLYP (vide infra).

From Table 2, it is evident that the  $C-X\cdots O$  contacts are rather linear. The  $C-X\cdots O$  angles are estimated to be within a range from  $150^\circ$  to  $175^\circ$  at both levels of theory, which in general fall into the main statistical scope of halogen bonding found in biological molecules ( $140\text{--}170^\circ$ ).<sup>11</sup> The directionality of the interaction similar to hydrogen bonding accords with the anisotropic distribution of electrostatic potential of halogen atoms with the presence of a positive cap along the  $C-X$  axis, as illustrated in Figure 3. Of note are that striking departures from

linearity of the interactions in some cases take place ( $\angle(C-X\cdots O) < 160^\circ$ ), whereas in most small halogen-bonded complexes, the interactions are indeed found to be essentially linear ( $\angle(R-X\cdots O) \approx 180^\circ$ ).<sup>30,31</sup> The noticeably greater variation in the geometry of halogen bonding in biological molecules compared to that observed in small model systems is not surprising, considering the much increased complexity of biomacromolecules. The surrounding proteins thus would have a pronounced effect on halogen bonding geometries. On the other hand, the  $C-O\cdots X$  angles are predicted to be larger than  $120^\circ$  for all systems studied herein, except for 1PMN and

1QYE, in which the C—O $\cdots$ X angles are close to 90°. In these two cases, it is the  $\pi$  electron density rather than the O lone pair electrons that serves as electron donor. In fact, the perpendicular approach of halogens toward O=C oxygens of peptide bonds occurs frequently in biological molecules.<sup>11</sup> Generally, the calculated C—X $\cdots$ O and C—O $\cdots$ X angles compare relatively well to the values in X-ray structures. The deviation of the structures of the optimized full models from their X-ray structures can be quantified by the computations of rmsd values. It can be seen from Table 2 that the calculated rmsd values for the present models are around the scale of X-ray diffraction resolutions of studied protein crystals, indicating that the optimized model structures should be reliable. This can be visualized from superposing the X-ray structures and the optimized model structures of 1PMN, 1ZOH, and 1S9J shown in Figure 5 as examples. In addition, given that the rmsd values for the MPWLYP method are remarkably close to those for B3LYP, the structures optimized via the two approaches should be highly identical.

Also included in Table 2 are the binding energies between the ligands and protein residues, i.e., halogen bonding energies, computed at both levels. It is clear that most of the contacts between halogen and oxygen atoms are shown to be attractive interactions. But for the systems of 1PMN and 1QYE, regardless of the methods used, positive values of the binding energies are attained, resulting in repulsive interactions in these two models. This is not unexpected, taking into account of the substantially small size of electrostatic positive crown of chlorine in relation to bromine and iodine, as displayed in Figure 3. On the basis of these, most of the Cl $\cdots$ O interactions in biomolecules appear to be extremely weak or even repulsive. By performing single-point calculations, we estimate binding energies to be  $-0.23$  to  $-1.96$  kcal/mol by using the B3LYP method and  $-0.98$  to  $-3.22$  kcal/mol at the MPWLYP level. Halogen bonding interactions seem to become comparable in magnitude to the well-studied hydrogen bonds, especially for the more polarizable halogens. In view of the directionality and strength, halogen bonding would be a novel interaction in drug design. Such interaction, however, has to a large degree been unrecognized in the world of biology. It is worth mentioning that the MPWLYP method predicts more negative binding energies in comparison with B3LYP, albeit the structures optimized with the two approaches are highly identical (vide supra). For instance, the interaction in the system of 1H1R is shown to be repulsive when using the B3LYP method, while the binding energy of this system calculated at the MPWLYP level amounts to  $-0.98$  kcal/mol. In contrast, the rmsd values of the full model of this system are insensitive to the methods applied (1.944 vs 1.966). The better performance of MPWLYP has been substantiated in our recent benchmark study of halogen bonding in small model molecules.<sup>63</sup> Not surprisingly, the Cl $\cdots$ O interaction in 1H1R is evaluated to be much stronger than that in 1PMN, which can be attributed to the negative charge-assisted halogen bond presented in 1H1R. From the data of these two systems tabulated in Table 2, a trend can be observed that the stronger the interaction, the shorter the Cl $\cdots$ O distance, which has been well documented in small halogen-bonded complexes. Nonetheless, in the systems of 1S9J and 1S9I, the interactions exhibit a contrary kind of behavior as those in 1PMN and 1H1R. This irregular variation of halogen bonding in biomolecular systems also mirrors the considerably enhanced complexity of biomacromolecules.

The thyroid hormones, such as thyroxine (T4) and triiodothyronine (T3), are tyrosine-based hormones produced by thyroid

**Table 3.** Geometrical and Energetic Properties of Four Systems at the MPWLYP Level

systems	IC <sub>50</sub>	rmsd (QM) 6-31G(d)	$\Delta E$ (kcal/mol)	
			-311+G(d)	Lan12dz
1H1Q	1.0 $\mu$ M	2.864	-5.83	-6.89
1H1R	2.3 $\mu$ M	1.966	-0.98	—
1H1R-Br	—	—	-5.00	-2.59
1H1R-I	—	—	—	-6.71

gland. An important component in the synthesis is iodine. The thyroid hormones are essential to proper development and differentiation of all cells of the human body.<sup>74</sup> Particularly, synthroid (levothyroxine sodium), the typical band of T4, has now been one of the most popular prescription drugs in the United States. According to our present survey, a huge number of short I $\cdots$ O contacts, which occupy approximately 50% of all statistical I $\cdots$ O interactions between these hormones and their associated proteins, have been identified. One of the systems, 1NQ2, was selected to investigate in this work. Table 2 shows that for this system the I $\cdots$ O interaction from T3 to its receptor hTR $\beta$  is calculated to be quite linear ( $\angle(\text{C}-\text{X}\cdots\text{O}) \approx 170^\circ$ ), and the interaction energy is as high as  $-3.22$  kcal/mol at the MPWLYP/lan2dz level. Given the linearity as well as the stability, the I $\cdots$ O interactions must play pivotal roles in the recognition of the hormones by their cognate proteins, which supports previous perspectives of Ho and co-workers.<sup>11</sup>

We then focus our attention on the system of 1H1R. The X-ray structure of CDK2-cyclinA3 in complex with the inhibitor NU6094 (**7**),<sup>54</sup> which in comparison with **2** the chlorine substituent is superseded by H, is also available (PDB code 1H1Q<sup>54</sup>). Figure 6a displays the superposition of the models in the X-ray structures of 1H1R and 1H1Q. It has been stated by Newell and co-workers that the mode of inhibitor binding of **2** was identical to **7**, while the affinity of **2** for CDK2 was not improved over **7** (see Table 3).<sup>54</sup> To provide a detailed understanding of the interactions between the inhibitors and protein residue Asp86, the model structure of 1H1Q was optimized at the ONIOM(MPWLYP:AMBER) level. Also considered at the same level of theory are other two systems, 1H1R-Br and 1H1R-I, i.e., the Cl atom in the 1H1R system is substituted by Br and I, respectively. To ensure that the data of the four systems are comparable, calculations with the lan12dz basis set were also performed on 1H1Q and 1H1R-Br. Table 3 lists the geometrical and energetic characteristics for these systems of interest. It can be seen that the strength of the interactions between the ligands and residue Asp 86 decreases in the following order  $\text{H} \approx \text{I} > \text{Br} > \text{Cl}$ , which agrees with the properties of halogen bonding in small molecules noted above. The binding energies of 1H1R-Br and 1H1R-I are shown to be markedly greater in magnitude than that of 1H1R, whereas the optimized structures of the full models are almost identical for these systems (cf Figure 6b). In this regard, the potency of inhibitor **2** may be much increased when displacing the Cl atom to Br or I. This would be, of course, concluded with great caution and requires further experimental verifications. From Figure 6, it is apparent that the conformation of **7** in the active site varies to some degree as compared to **2** and other two halogenated molecules. Because the mode of inhibitor binding of **2** was demonstrated to be similar to **7**, the interactions between the ligands and residue Asp86 appear to play a major role in orienting the ligands inside the active site. To sum up, halogen substituents not only interact with backbone or side chain oxygen atoms of protein residues but affect the conformations of parent compounds. These would make halogen bonding a novel or at least a potential tool for designing protein inhibitors

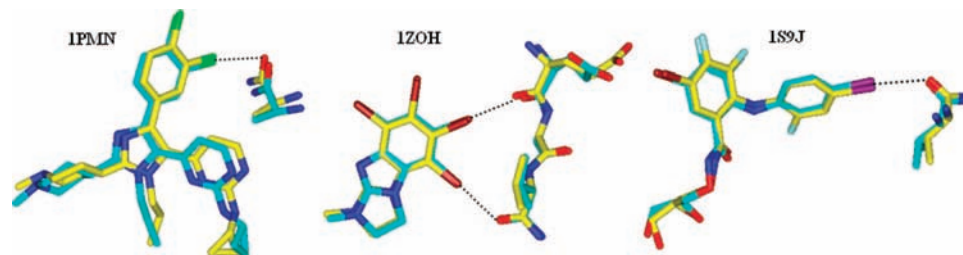


**Figure 5.** Superpositions of X-ray structures (yellow) and ONIOM(B3LYP/AMBER) optimized structures (cyan) of IPMN, IZOH, and IS9J.

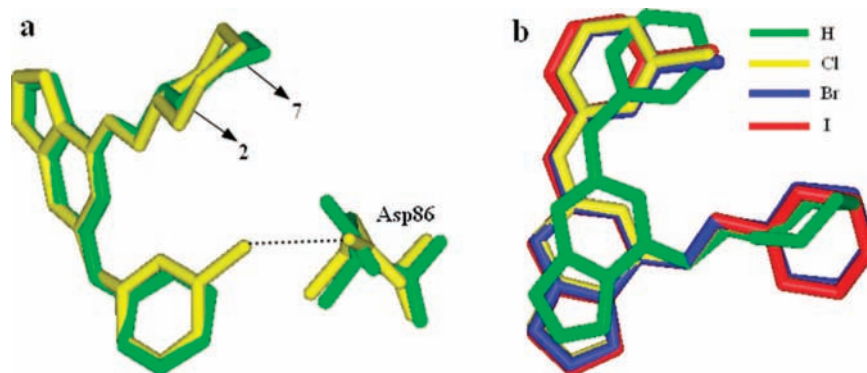


**Figure 6.** (a) Superposition of the full models of X-ray structures of 1H1R and 1H1Q. (b) Superposition of four ligand structures in model systems optimized at the ONIOM(MPWLYP/AMBER) level.

and drugs. It should be pointed out that the statements presented here are based only on a single system and thus have great limitations. Nonetheless, the conclusions derived from the single system may cast some light on the important role of halogen bond in rational drug design. In fact, the introduction of halogen atoms in ligands also causes many other factors that influence inhibitor recognition and binding, such as specificity surface and hydrophobic effect.<sup>17</sup>

## Conclusions

Despite the limited systems studied here, halogen bonding was demonstrated to play an important role in inhibitor recognition and binding, at least by protein kinases. Calculations on the basis of the ONIOM-based QM/MM scheme unravel that the distances between the halogen and oxygen atoms are predicted to be much shorter than the van der Waals radius sums. Single-point energy computations carried out on the full models show that the interactions are comparable in strength to classical hydrogen bonds. Moreover, we found that the strength of the interactions decreases in the order  $H \approx I > Br > Cl$ . These results are in good agreement with the properties detected within small model complexes associated with halogen bonding. However, a notably greater variation in the geometry and energetics of halogen bonding in biomolecular systems compared to those in small molecules is observed, which can be rationalized by the conspicuously increased complexity of biomolecules. A further analysis of the interactions indicates that halogen bonding interactions are responsible for the different conformation of the molecules in the active site. The computational findings in this work can be readily extended to other enzyme-ligand systems so that halogen bonding, which has long been underappreciated in the field of biology, would enable the discovery of new, potent enzyme inhibitors. It should be pointed out here that halogen bonding in biological systems seems to be somewhat weak according to our calculations, especially for the lighter halogens, while hydrogen bonding interactions of biological importance, indeed, have a wide range of stabilization

energy (1–20 kcal/mol).<sup>75,76</sup> However, the linear preference of this type of nonbonded interaction and the special chemical properties of halogen atoms should render halogen bonding very useful in drug design, e.g., inducing significant conformational perturbations, particularly in nucleic acids.<sup>16</sup>

As a result of the unique features of halogen bonding, present molecular dynamic simulations, which rely primarily upon empirical force fields that in general do not explicitly account for the anisotropic distribution of charge density, appear to be not appropriate for describing halogen bonding. Developing accurate and reliable force fields for halogen bonding is currently underway in our laboratory.

**Acknowledgment.** This work was supported by the National Natural Science Foundation of China (20572117), the Hi-Tech Research and Development Program of China (2006AA02Z336), and the Postdoctoral Science Foundation of China (20080440664).

**Supporting Information Available:** Summary of the structures associated with  $X \cdots O$  contacts from a survey of the Protein Data Bank (December 2008 release). This material is available free of charge via the Internet at <http://pubs.acs.org>.

## References

- (1) Metrangolo, P.; Resnati, G. *Halogen Bonding: Fundamentals and Applications*; Springer: Berlin, 2008.
- (2) Metrangolo, P.; Resnati, G. Halogen bonding: a paradigm in supramolecular chemistry. *Chem.-Eur. J.* **2001**, *7*, 2511–2519.
- (3) Metrangolo, P.; Neukirch, H.; Pilati, T.; Resnati, G. Halogen bonding based on recognition processes: a world parallel to hydrogen bonding. *Acc. Chem. Res.* **2005**, *38*, 386–395, and references therein.
- (4) Metrangolo, P.; Resnati, G.; Pilati, T.; Liantonio, R.; Meyer, F. Engineering functional materials by halogen bonding. *J. Polym. Sci., Part A: Polym. Chem.* **2007**, *45*, 1–15, and references therein.
- (5) Metrangolo, P.; Meyer, F.; Pilati, T.; Resnati, G.; Terraneo, G. Halogen bonding in supramolecular chemistry. *Angew. Chem., Int. Ed.* **2008**, *47*, 6114–6127, and references therein.
- (6) Metrangolo, P.; Resnati, G. Halogen versus hydrogen. *Science*. **2008**, *321*, 918–919.

- (7) Rosokha, S. V.; Neretin, I. S.; Rosokha, J. Y.; Hecht, J.; Kochi, K. K. Charge-transfer character of halogen bonding: molecular structures and electronic spectroscopy of carbon tetrabromide and bromoform complexes with organic  $\sigma$ - and  $\pi$ -donors. *Heteroatom. Chem.* **2006**, *17*, 449–459.
- (8) Rissanen, K. Halogen bonded supramolecular complexes and networks. *CrystEngComm* **2008**, *10*, 1107–1113.
- (9) Aakeröy, C. B.; Fasulo, M.; Schultheiss, N.; Desper, J.; Moore, C. Structural competition between hydrogen bonding and halogen bonding. *J. Am. Chem. Soc.* **2007**, *129*, 13772–13773.
- (10) Bouchmella, K.; Boury, B.; Dutremez, S. G.; van der Lee, A. Molecular assemblies from imidazolyl-containing haloalkenes and haloalkynes: competition between hydrogen and halogen bonding. *Chem.—Eur. J.* **2007**, *13*, 6130.
- (11) Auffinger, P.; Hays, F. A.; Westhof, E.; Ho, P. S. Halogen bonding in biological molecules. *Proc. Natl. Acad. Sci. U.S.A.* **2004**, *101*, 16789–16794.
- (12) Ghosh, M.; Meerts, I. A. T. M.; Cook, A.; Bergman, A.; Brouwer, A.; Johnson, L. N. Structure of human transthyretin complexed with bromophenols: a new mode of binding. *Acta. Crystallogr., Sect. D: Biol. Crystallogr.* **2001**, *56*, 1085–1095.
- (13) Jiang, Y.; Alcaraz, A. A.; Chem, J. M.; Kobayashi, H.; Lu, Y. J.; Snyder, J. P. Diastereomers of dibromo-7-*epi*-10-deacetylcephalomanine: crowded and cytotoxic taxanes exhibit halogen bonds. *J. Med. Chem.* **2006**, *49*, 1891–1899.
- (14) Gopalakrishnan, B.; Aparna, V.; Ravi, J. J. M.; Desiraju, G. R. A virtual screening approach for thymidine monophosphate kinase inhibitors as anti-tubercular agents based on docking and pharmacophore models. *J. Chem. Inf. Model.* **2005**, *45*, 1101–1108.
- (15) Himmel, D. M.; Das, K.; Clark, A. D.; Hughes, S. H.; Benjahad, A.; Oumouch, S.; Guillemont, J.; Coupa, S.; Poncelet, A.; Csoka, I.; Meyer, C.; Andries, K.; Nguyen, C. H.; Grierson, D. S.; Arnold, E. Crystal structures for HIV-1 reverse transcriptase in complex with three pyridinone derivatives: a new class of non-nucleoside inhibitors effective against a broad range of drug-resistant strains. *J. Med. Chem.* **2005**, *48*, 7582–7591.
- (16) Voth, A. R.; Hays, F. A.; Ho, P. S. Directing macromolecular conformation through halogen bonds. *Proc. Natl. Acad. Sci. U.S.A.* **2007**, *104*, 6188–6193.
- (17) Voth, A. R.; Ho, P. S. The role of halogen bonding in inhibitor recognition and binding by protein kinases. *Curr. Top. Med. Chem.* **2007**, *7*, 1336–1348.
- (18) Tawarada, R.; Seio, K.; Sekine, M. Synthesis and properties of oligonucleotides with iodo-substituted aromatic aglycons: investigation of possible halogen bonding base pairs. *J. Org. Chem.* **2008**, *73*, 383–390.
- (19) Marsden, B. D.; Knapp, S. Doing more than just the structure—structural genomics in kinase drug discovery. *Curr. Opin. Chem. Biol.* **2008**, *12*, 40–45.
- (20) Levesque, D.; Beaudoin, J. D.; Roy, S.; Perreault, J. P. In vitro selection and characterization of RNA aptamers binding thyroxine hormone. *Biochem. J.* **2007**, *403*, 129–138.
- (21) Bondi, A. van der Waals volumes and radii. *J. Phys. Chem.* **1964**, *68*, 441–451.
- (22) Manning, G.; Whyte, D. B.; Martinez, R.; Hunter, T.; Sudarsanam, S. The protein kinase complement of the human genome. *Science* **2002**, *298*, 1912–1934.
- (23) Cohen, P. Protein kinases—the major drug targets of the twenty-first century. *Nat. Rev. Drug. Discovery* **2001**, *1*, 309–315.
- (24) Bogoyevitch, M. A. The isoform-specific functions of the c-Jun N-terminal kinases (JNKs): differences revealed by gene targeting. *Bioessays* **2006**, *28*, 923–934.
- (25) Knockaert, M.; Greengard, P.; Meijer, L. Pharmacological inhibitors of cyclin-dependent kinases. *Trends. Pharmacol. Sci.* **2002**, *23*, 417–425.
- (26) Nobel, M. E.; Endicott, J. A.; Johnson, L. N. Protein kinase inhibitors: insights into drug design from structure. *Science* **2004**, *303*, 1800–1805.
- (27) Valerio, G.; Raos, G.; Meille, S. V.; Metrangolo, P.; Resnati, G. Halogen bonding in fluoroalkylhalides: a quantum chemical study of increasing fluorine substitution. *J. Phys. Chem. A* **2000**, *104*, 1617–1620.
- (28) Karpfen, A. Charge-transfer complexes between  $\text{NH}_3$  and the halogens  $\text{F}_2$ ,  $\text{Cl}_2$ , and  $\text{Cl}_2$ : an ab initio study on the intermolecular interaction. *J. Phys. Chem. A* **2000**, *104*, 6871–6879.
- (29) Alkorta, I.; Rozas, J.; Elguero, J. Charge-transfer complexes between dihalogen compounds and electron donors. *J. Phys. Chem. A* **1998**, *102*, 9278–9285.
- (30) Wang, W. Z.; Wong, N.-B.; Zheng, W. X.; Tian, A. M. Theoretical study on the blue-shifting halogen bond. *J. Phys. Chem. A* **2004**, *108*, 1799–1805.
- (31) Zou, J. W.; Jiang, Y. J.; Guo, M.; Hu, G. X.; Zhang, B.; Liu, H. C.; Yu, Q. S. Ab initio study of the complexes of halogen-containing molecules  $\text{RX}$  ( $\text{X} = \text{Cl}, \text{Br}, \text{and I}$ ) and  $\text{NH}_3$ : towards understanding the nature of halogen bonding and the electron-accepting propensities of covalently bonded halogen atoms. *Chem.—Eur. J.* **2005**, *11*, 740–751.
- (32) Lu, Y. X.; Zou, J. W.; Wang, H. Q.; Yu, Q. S.; Zhang, H. X.; Jiang, Y. J. Ab initio investigation of the complexes between bromobenzene and several electron donors: some insights into the magnitude and nature of halogen bonding interactions. *J. Phys. Chem. A* **2007**, *111*, 10781–10788.
- (33) Bilewicz, E.; Grabowski, S. J. Cooperativity halogen bonding effect—ab initio calculations on  $\text{H}_2\text{CO}\cdots(\text{ClF})_n$  complexes. *Chem. Phys. Lett.* **2006**, *427*, 51–55.
- (34) Awwadi, F. F.; Willett, R. D.; Peterson, K. A.; Twamley, B. The nature of halogen $\cdots$ halogen synthons: crystallographic and theoretical studies. *Chem.—Eur. J.* **2006**, *12*, 8152–8161.
- (35) Riley, K. E.; Merz, K. M. Insights into the strength and origin of halogen bonding: the halobenzene—formaldehyde dimer. *J. Phys. Chem. A* **2007**, *111*, 1688–1684.
- (36) Riley, K. E.; Hobza, P. Investigations into the nature of halogen bonding including symmetry adapted perturbation theory analyses. *J. Chem. Theory Comput.* **2008**, *4*, 232–243.
- (37) Wang, W. Z.; Hobza, P. Origin of the X-Hal ( $\text{Hal} = \text{Cl}, \text{Br}$ ) bond-length change in the halogen-bonded complexes. *J. Phys. Chem. A* **2008**, *112*, 4114–4120.
- (38) Shishkin, O. V. Evaluation of true energy of halogen bonding in the crystals of halogen derivatives of trityl alcohol. *Chem. Phys. Lett.* **2008**, *458*, 96–100.
- (39) Li, Q. Z.; Lin, Q. Q.; Li, W. Z.; Cheng, J. B.; Suo, J. Z. Cooperativity between the halogen bond and the hydrogen bond in  $\text{H}_3\text{N}\cdots\text{XY}\cdots\text{HF}$  complexes ( $\text{X}, \text{Y} = \text{F}, \text{Cl}, \text{Br}$ ). *ChemPhysChem* **2008**, *9*, 2265–2269.
- (40) Alkorta, M.; Blanco, F.; Solimannejia, M.; Elguero, J. Competition of hydrogen bonds and halogen bonds in complexes of hypohalous acids with nitrogenated bases. *J. Phys. Chem. A* **2008**, *112*, 10856–10863.
- (41) Palusiak, M.; Grabowski, S. Do intramolecular halogen bonds exist? Ab initio calculations and crystal structures' evidences. *Struct. Chem.* **2008**, *19*, 5–11.
- (42) Singh, U. C.; Kollman, P. A. A combined ab initio quantum mechanical and molecular mechanical method for carrying out simulations on complex molecular systems: applications to the  $\text{CH}_3\text{Cl} + \text{Cl}^-$  exchange reaction and gas phase protonation of polyethers. *J. Comput. Chem.* **1986**, *7*, 718–730.
- (43) Svensson, M.; Humbel, S.; Froese, R. D. J.; Matsubara, J.; Siber, S.; Morokuma, K. ONIOM: a multilayered integrated MO + MM method for geometry optimizations and single point energy predictions. a test for Diels–Alder reactions and  $\text{Pt}(\text{t-Bu})_3)_2 + \text{H}_2$  oxidative addition. *J. Phys. Chem.* **1996**, *100*, 19357–19363.
- (44) Dapprich, S.; Komáromi, I.; Byun, S.; Morokuma, K.; Frisch, M. J. A new ONIOM implementation in Gaussian 98. Part I. the calculations of energies, gradients, vibrational frequencies, and electric field derivatives. *J. Mol. Struct.: THEOCHEM* **1999**, *461*, 1–21.
- (45) Vreven, T.; Morokuma, K.; Frakas, O.; Schlegel, H. B.; Frisch, M. T. Geometry optimization with QM/MM, ONIOM, and other combined methods. I. Microiterations and constraints. *J. Comput. Chem.* **2003**, *24*, 760–769.
- (46) Xiong, Y.; Lu, H. L.; Zhan, C. G. Dynamic structures of phosphodiesterase-5 active site by combined molecular dynamics simulations and hybrid quantum mechanical/molecular mechanical calculations. *J. Comput. Chem.* **2008**, *29*, 1259–1267.
- (47) Shi, Q.; Meroueh, S. O.; Fisher, J. F.; Mobashery, S. Investigation of the mechanism of the cell wall DD-carboxypeptidase reaction of penicillin-binding protein 5 of *Escherichia coli* by quantum mechanics/molecular mechanics calculations. *J. Am. Chem. Soc.* **2008**, *130*, 9293–9303.
- (48) Carvalho, A. T. P.; Fernandes, P. A.; Ramos, M. J. Theoretical study of the unusual protonation properties of the active site cysteines in thioredoxin. *J. Phys. Chem. B* **2006**, *110*, 5758–5761.
- (49) Torrent, M.; Vreven, T.; Musaev, D. G.; Morokuma, K.; Farkas, Ö.; Schlegel, H. B. Effects of the protein environment on the structure and energetics of active sites of metalloenzymes. ONIOM study of methane monooxygenase and ribonucleotide reductase. *J. Am. Chem. Soc.* **2002**, *124*, 192–193.
- (50) Meroueh, S. O.; Fisher, J. F.; Schlegel, H. B.; Mobashery, S. Ab initio QM/MM study of class  $\beta$ -lactamase acylation: dual participation of Glu166 and Lys73 in a concerted base promotion of Ser70. *J. Am. Chem. Soc.* **2005**, *127*, 15397–15407.
- (51) Kwiecien, R. A.; Khavrutski, L. V.; Musaev, D. G.; Morokuma, K.; Banerjee, R.; Paneth, P. Computational insights into the mechanism of radical generation in  $\text{B}_{12}$ -dependent methylmalonyl-CoA mutase. *J. Am. Chem. Soc.* **2006**, *128*, 12871292.
- (52) Lundberg, M.; Morokuma, K. Protein environment facilitates  $\text{O}_2$  binding in non-heme iron enzyme. An insight from ONIOM calcula-



- tions on isopenicillin N synthase (IPNS). *J. Phys. Chem. B* **2007**, *111*, 9380–9389.
- (53) Scapin, G.; Patel, S. B.; Lisnock, J.; Becker, J. W.; LoGrasso, P. V. The structure of JNK3 in complex with small molecule inhibitors: structural basis for potency and selectivity. *Chem. Biol.* **2003**, *10*, 705–712.
- (54) Davies, T. G.; Bentley, J.; Arris, C. E.; Boyle, F. T.; Curtin, N. J.; Endicott, J. A.; Gibson, A. E.; Golding, B. T.; Griffin, R. J.; Hardcastle, L. R.; Jewsbury, P.; Johnson, L. N.; Mesguiche, V.; Newell, D. R.; Nobel, M. E. M.; Tucker, J. A.; Wang, L.; Whitfield, H. Structure-based design of a potent purine-based cycli-dependent kinase inhibitor. *Nat. Struct. Biol.* **2002**, *9*, 745–749.
- (55) Battistutta, R.; Mazzorana, M.; Sarno, S.; Kazimierczuk, Z.; Zanotti, G.; Pinna, L. A. Inspecting the structure–activity relationship of protein kinase CK2 inhibitors derived from tetrabromo-benzimidazole. *Chem. Biol.* **2005**, *12*, 1211–1219.
- (56) Ohren, J. F.; Chen, H.; Pavlovsky, A.; Whitehead, C.; Zhang, E.; Kuffa, P.; Yan, C.; McConnell, P.; Spessard, C.; Banotai, C.; Mueller, W. T.; Delaney, A.; Omer, C.; Sebolt-Leopold, J.; Dudley, D. T.; Leung, I. K.; Flamme, C.; Warmus, J.; Kaufman, M.; Barrett, S.; Teclé, H.; Hasemann, A. Structures of human MAP kinase kinase 1 (MEK1) and MEK2 describe novel noncompetitive kinase inhibition. *Nat. Struct. Mol. Biol.* **2004**, *11*, 1192–1197.
- (57) Soldano, K. L.; Jivan, A.; Nicchitta, C. V.; Gewirth, D. T. Structure of the N-terminal domain of GRP94. *J. Biol. Chem.* **2003**, *279*, 48330–48338.
- (58) Mueller-Dieckmann, C.; Ritter, H.; Haag, F.; Koch-Nolte, K.; Schulz, G. Z. Structure of the Ecto-ADP-ribosyl transferase ART2.2 from rat. *J. Mol. Biol.* **2002**, *322*, 687–696.
- (59) Schumacher, M. A.; Scott, D. M.; Mathews, I. I.; Ealick, S. E.; Roos, D. S.; Ullman, B.; Brennan, R. G. Crystal structures of *Toxoplasma gondii* adenosine kinase reveal a novel catalytic mechanism and prodrug binding. *J. Mol. Biol.* **2000**, *298*, 875–893.
- (60) Huber, B. R.; Sandler, B.; West, B. L.; Lima, S. T. C.; Nauyen, H. T.; Apriletti, J. W.; Baxter, J. D.; Fletterick, R. J. Two resistance to thyroid hormone mutants with impaired hormone binding. *Mol. Endocrinol.* **2003**, *17*, 643–652.
- (61) Becke, A. D. Density-functional exchange-energy approximation with correct asymptotic behavior. *Phys. Rev. A* **1988**, *38*, 3098–3100.
- (62) Lee, C.; Yang, W.; Parr, R. G. Development of the Colle–Salvetti correlation-energy formula into a functional of the electron density. *Phys. Rev. B* **1998**, *37*, 785–789.
- (63) Adamo, C.; Barone, V. Exchange functionals with improved long-range behavior and adiabatic connection methods without adjustable parameters: the mPW and mPW1PW models. *J. Chem. Phys.* **1998**, *108*, 664–675.
- (64) Lu, Y. X.; Zou, J. W.; Fan, J. C.; Zhao, W. N.; Jiang, Y. J.; Yu, Q. S. Ab initio calculations on halogen-bonded complexes and comparison with density functional methods. *J. Comput. Chem.* **2009**, *30*, 725–732.
- (65) Cornell, W. D.; Cieplak, P.; Bayly, C. I.; Gould, I. R. L.; Merz, J. K. M.; Ferguson, D. M.; Spellmeyer, D. C.; Fox, T.; Caldwell, J. W.; Kollman, P. A. A second generation force field for the simulation of proteins, nucleic acids, and organic molecules. *J. Am. Chem. Soc.* **1995**, *117*, 5179–5197.
- (66) Wang, J.; Wolf, R. M.; Caldwell, J. W.; Kollman, P. A.; Case, D. A. Developing and testing of a general amber force field. *J. Comput. Chem.* **2004**, *25*, 1157–1174.
- (67) Boys, S. F.; Bernardi, F. The calculation of small molecular interactions by the differences of separate total energies. some procedures with reduced errors. *Mol. Phys.* **1970**, *19*, 553–566.
- (68) Frisch, M. J.; Trucks, G. W.; Schlegel, H. B.; Scuseria, G. E.; Robb, M. A.; Cheeseman, J. R.; Zakrzewski, V. G.; Montgomery, J. A., Jr.; Stratmann, R. E.; Burant, J. C.; Dapprich, S.; Millam, J. M.; Daniels, A. D.; Kudin, K. N.; Strain, M. C.; Farkas, O.; Tomasi, J.; Barone, V.; Cossi, M.; Cammi, R.; Mennucci, B.; Pomelli, C.; Adamo, C.; Clifford, S.; Ochterski, J.; Petersson, G. A.; Ayala, P. Y.; Cui, Q.; Morokuma, K.; Malick, D. K.; Rabuck, A. D.; Raghavachari, K.; Foresman, J. B.; Cioslowski, J.; Ortiz, J. V.; Stefanov, B. B.; Liu, G.; Liashenko, A.; Piskorz, P.; Komaromi, I.; Gomperts, R.; Martin, R. L.; Fox, D. J.; Keith, T.; Al-Laham, M. A.; Peng, C. Y.; Nanayakkara, A.; Gonzalez, C.; Challacombe, M.; Gill, P. M. W.; Johnson, B. G.; Chen, W.; Wong, M. W.; Andres, J. L.; Head-Gordon, M.; Replogle, E. S.; Pople, J. A. *Gaussian 03*; Gaussian, Inc.: Wallingford, CT, 2003.
- (69) Trogden, G.; Murray, J. S.; Concha, M. C. Molecular surface electrostatic potentials and anesthetic activity. *J. Mol. Model.* **2007**, *13*, 313–318.
- (70) Politzer, P.; Lane, P.; Concha, M. C.; Ma, Y.; Murray, J. S. An overview of halogen bonding. *J. Mol. Model.* **2007**, *13*, 305–311.
- (71) Clark, T.; Hennemann, M.; Murray, J. S.; Politzer, P. Halogen bonding: the  $\sigma$ -hole. *J. Mol. Model.* **2007**, *13*, 291–296.
- (72) Murray, J. S.; Lane, P.; Clark, T.; Politzer, P.  $\sigma$ -Hole bonding: molecules containing group VI atoms. *J. Mol. Model.* **2007**, *13*, 1033–1038.
- (73) Murray, J. S.; Lane, P.; Politzer, P. A predicted new type of directional noncovalent interaction. *Int. J. Quantum Chem.* **2007**, *107*, 2286–2292.
- (74) Refetoff, S. Resistance to thyroid hormone. *Clin. Lab. Med.* **1993**, *13*, 563–581.
- (75) Jurecka, P.; Sponer, J.; Cerny, J.; Hobza, P. Benchmark database of accurate (MP2 and CCSD(T) complete basis set limit) interaction energies of small model complexes, DNA base pairs and amino acid pairs. *Phys. Chem. Chem. Phys.* **2006**, *8*, 1985–1993.
- (76) Wang, Z. X.; Wu, C.; Lei, H. X.; Duan, Y. Accurate ab initio study on the hydrogen-bond pairs in protein secondary structures. *J. Chem. Theory. Comput.* **2007**, *3*, 1527–1537.

JM9000133